Mean Densities in Dynamic Mathematical Two-phase Flow Models

J. Bonilla[1], L.J. Yebra[1] and S. Dormido[2]

Abstract: This paper presents and discusses a mean densities method applied to a steam-water two-phase flow mathematical model which uses a finite volume method and a staggered grid for discretizing a rigid volume in control volumes, where the thermodynamic properties are calculated. This method is based on the concepts of uniform pressure among all the control volumes and mean density in each control volume, allowing smooth thermodynamic properties, hence avoiding discontinuity at phase boundaries. This method wipes out the chattering problem due to the continuous and differentiable modelling of density and its partial derivatives, which leads to faster simulations and increases the simulation performance.

Keywords: Chattering, two-phase flow, modelling and simulation, mean densities, finite volume method.

1   Introduction

Mean densities is a mathematical model for the calculation of two-phase flow steam-water models thermodynamic properties in a rigid volume. The rigid volume is discretized in control volumes using the finite volume method (FVM) [Patankar (1980)] and the staggered grid method [Harlow and Welch (1965)]. In each control volume the thermodynamic properties are calculated using mean densities. Mean densities is based on [Casella (2006)] with slightly variations, which are discussed in this paper.

The aim of the development of this method is mainly due to chattering problems in dynamic simulation. The real system modelled, where the chattering problem arises, is the PSA-CIEMAT (Plataforma Solar de Almería - Centro de Investigaciones Energéticas MedioAmbientales y Tecnológicas, a Spanish government

---

[1] PSA-CIEMAT, Plataforma Solar de Almería - Centro de Investigaciones Energéticas, MedioAmbientales y Tecnológicas, 04200 Tabernas (Almería), Spain.
[2] UNED, Universidad Nacional de Educación a Distancia, Escuela Técnica Superior de Ingeniería Informática, 28040, Madrid, Spain.

research center) DISS (DIrect Solar Steam) test facility, a parabolic-trough solar power plant. The heat transfer fluid in the DISS test facility is steam and water in two-phase flow. This technology is known as DSG (Direct Steam Generation) as a separate steam generator is unnecessary to produce steam (see Fig. 1 [Zarza (2000)] for an illustration of the parabolic-trough principle). One of the several different solar thermal concentrating technologies available is the parabolic-trough technology. Parabolic-Trough Collectors (PTCs) are solar concentrators which convert the direct solar radiation into thermal energy, heating the heat transfer fluid up to around 675 K. Their high working temperature makes PTCs suitable for supplying heat to industrial processes, replacing traditional fossil fuels [Kutshcer, Davenport, Dougherty, Gee, Masterson, and Kenneth (1982)]. A PTC is basically a mirror in the form of a parabola, which collects solar radiation and concentrates it on the absorber tube located in the parabola's focal line through which the heat transfer fluid is pumped, acquiring thermal energy from the solar radiation, see Fig. 1.

Fig. 2 shows a components diagram of the DISS test facility Modelica model developed in [Yebra (2006)] which was developed using Modelica [Modelica Association (2007a)] as the modelling language. Modelica has a standard library, Modelica.Media [Modelica Association (2007b)] which has been used for modelling the heat transfer fluid. Modelica.Media follows the IAPWS-IF97 formulation [IAPWS (1997)] for computing the thermodynamic properties of the medium. The thermal dynamics components used for the development of the dynamic Modelica model belongs to ThermoFluid library [Tummescheit, Eborn, and Wagner (2000);Eborn (2001)].
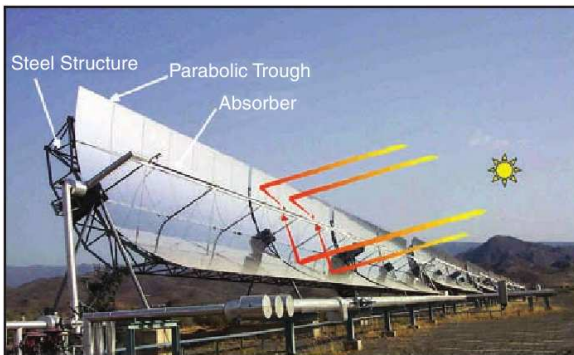

Figure 1: Main components and working principle of a PTC [Zarza (2000)]
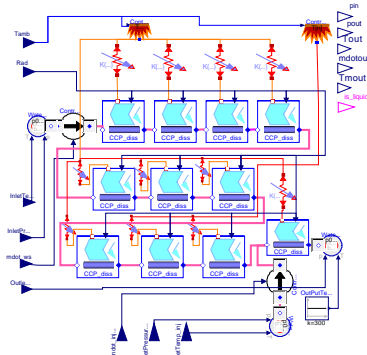
Figure 2: DISS test-bed facility Modelica model [Yebra (2006)]

Chattering produces high frequently oscilation between phase changes, due to discontinuities between phases that also produces a great number of state events, these

state events are computationally expensive, and finally this causes slow simulations and under certain circumstances they become unfeasible. The phase boundaries require special attention, even continuously differentiable trajectories of the state variables, pressure and especific enthalphy, in a control volume (CV) lead to small discontinuous density changes with discontinuous partial derivatives. The IAPWS-IF97 divides the formulation into regions allowing fast calculation of the steam-water thermodynamic properties, but it can lead to inconsistencies at the region boundaries, because there are small discontinuities between regions, these discontinuities have no physical reality, but are artifacts of the formulation method [The American Society of Mechanical Engineers (1999)]. While usually small, these discontinuities can be troublesome when the solver is trying to find a solution for a problem near a region boundary. Therefore, changes of the phase of fluids in a control volume must be implemented using a crossed function which restarts the integration process, this is required for efficiency and robutness, but it can lead to chattering.

The mathematical model to compute the state variables, pressure and specific enthalpy (p,h), of a two-phase flow model is shown in Eq. 1, where c is the speed of sound, ρ is density, V is the volume, $\left.\frac{\partial \rho}{\partial h}\right|_p$ and $\left.\frac{\partial \rho}{\partial p}\right|_h$ are the partial density derivatives with respect to the state variables, M_{net} is the the net mass flow and U_{net} is the net energy flow.

$$
\begin{pmatrix} \dot{p} \\ \dot{h} \end{pmatrix} = \frac{c^2}{\rho V} \begin{pmatrix} \rho + h\frac{\partial \rho}{\partial h}|_p & -\frac{\partial \rho}{\partial h}|_p \\ 1 - h\frac{\partial \rho}{\partial p}|_h & \frac{\partial \rho}{\partial p}|_h \end{pmatrix} \begin{pmatrix} M_{net} \\ U_{net} \end{pmatrix}.
\tag{1}
$$

When the phase boundaries are crossed, only the right hand side of the ODE changes discontinuously, the value of the state variables before and after the event are the same, they are C^0 continuous [Tummescheit (2002)]. But there are two different right-hand side of the Eq. 1, because the mathematical models of the thermodynamic properties are different in each phase, each right hand size provides a vector field which under certain circumstances gives a gradient that drives the solution towards the discontinuity.

Figure 3 shows a sketch of this behaviour, where two different gradients are shown in each phase, one-phase and two-phase (discontinuous-line arrows), and also where the state variables (p,h) (solved for each simulation step) are driven toward the discontinuity (the phase change curve, in this case the boiling curve h') represented by continuous-line arrows which describes a path with many phase changes due to the confrontation between both gradients.

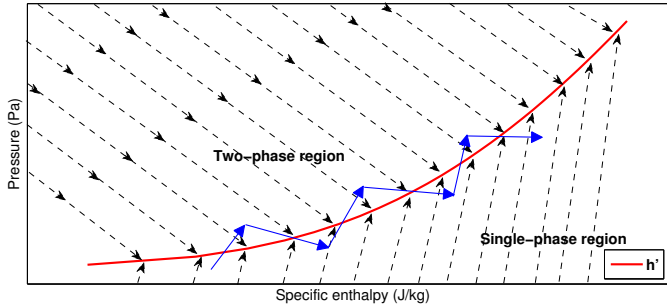The confrontation between both vector fields does not always happen, and this

Figure 3: Chattering sketch

is because also the mass flow afects. The density influences several terms in the momentum balance such that the mass flow changes with a phase change. Mass flow changes affect the right hand of the Eq. 1, and that affects the state variables (p,h) calculation.

The phase-change discontinuities are managed by the solver using a crossed function which restarts the integration process, this process is computationally expensive and it is repeated until the vector field gives a gradient which drives the solution outside the discontinuous region and increases consireably the simulation time.

There are two solutions for the chattering problem, mentioned in [Tummescheit (2002)].

- *Modify the momentum balance*. Using a moving boundary method where no spatial derivatives are taken over the phase boundaries and the grid is adjusted properly. This method gives good results [Heusser (1996)], its main drawback is the complexity of the resulting model.

- *Modify the thermodynamic properties to be continuous and differentiable at the region boundaries*. This method avoids simulation events and therefore chatttering in simulation. The thermodynamic properties involve in Eq. 1 are density, $\left.\frac{\partial \rho}{\partial h}\right|_p$ and $\left.\frac{\partial \rho}{\partial p}\right|_h$, hence these thermodynamic properties must be continuous and differentiable.

From a theoretical point of view the first solution is the appropiate one, because it is known that there are discontinuities in the thermodynamic properties at region boundaries and also they are controlled properly using discrete variables. However, the main disadvantage is that the resulting model is complex, therefore from a practical point of view the second solution is more feasible.

2   Conservation laws

For a quasi-unidimensional flow, such as a pipe [Anderson (1995); Roberts (2000)], the conservation laws, conservation of mass, momentum and energy, can be defined as Eq. 2, Eq. 3 and Eq. 4 respectively.

$$\frac{d(\rho A)}{dt} + \frac{\partial(\rho A v)}{\partial x} = 0, \tag{2}$$

$$\frac{d(\rho v A)}{dt} + \frac{\partial(\rho v^2 A)}{\partial x} = -A\frac{\partial p}{\partial x} - F_F - A\rho g\frac{\partial z}{\partial x}, \tag{3}$$

$$\frac{d(\rho(u+\frac{v^2}{2})A)}{dt} + \frac{\partial(\rho v(u+\frac{p}{\rho}+\frac{v^2}{2}A)}{\partial x} = -F_f v - A\rho v g\frac{\partial z}{\partial x} + \frac{\partial}{\partial x}(kA\frac{\partial T}{\partial x}). \tag{4}$$

Where, t is time, x is the spatial coordinate, ρ is density, v is velocity, A is area, p is pressure, $F_f = (1/2)\rho v|v|fS$, is the friction force per length, f is the Fanning friction factor, S is the circumference, g is the gravity force, u is the internal specific energy, z is the vertical displacement, k is the thermal conductivity and T is temperature.

3   Finite volume method

Considering a one-dimensional volume whose length is L, the partial differential equations (PDEs): mass, momentum and energy balance can be solved by the Finite Volume Method (FVM) [Patankar (1980)]. FVM has good properties with regards to maintaining the conserved quantities. The volume, in this case the pipe, is split in n control volumes, as shown in Fig. 4. For each one, the PDEs are approximated by ordinary differential equations (ODEs) where the staggered grid method [Harlow and Welch (1965)] is used. The mass and energy equations for the control volume V_j are integrated in $[x_{j-1}, x_j]$, hence the intensive properties are calculated in this interval, such as pressure (p) and specific enthalpy (h) which are the state variables. However, the momentum equation for the control volume V_j is integrated in $[x_{j-1} - l/2, x_j - l/2]$ where the fluxes are computed, such as the mass flow ($\dot{m}$). This approach claims to give better convergence properties by a better approximation of the pressure gradient.

The above-mentioned mathematical model is implemented in the ThermoFluid library. Particullarly in a pipe componet called PipeDD which belongs to the Components.Water.Pipes package.
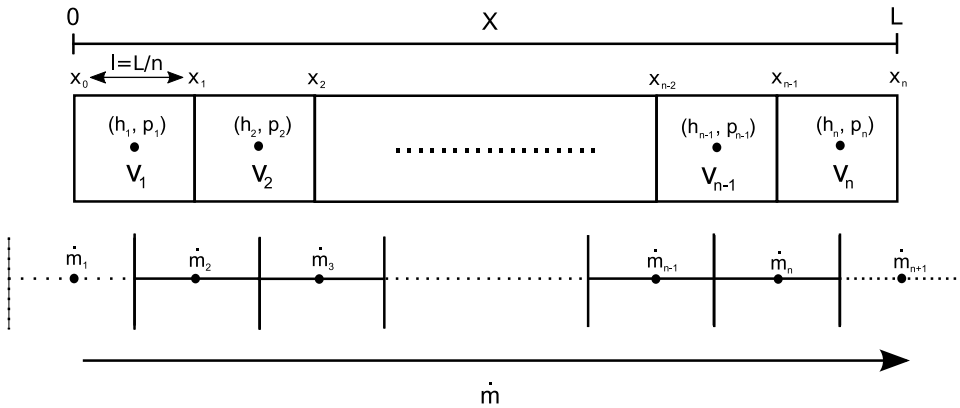
Figure 4: Finite volume method applied to volume V using a staggered grid

4   Finite-volume discretization of conservation laws

Applying the finite volume method, Eq. 2, Eq. 3 and Eq. 4 can be rewriten as Eq. 5, Eq. 6 and Eq. 7 respectively. This procedure is analogous to the process described in [Elmqvist, Tummescheit, and Otter (2003)], but for a collocated grid [Rhie and Chow (1983)] instead of a staggered grid which has been used in this work.

$$\frac{d(\bar{\rho}_j A_j l)}{dt} = \dot{m}_j + \dot{m}_{j+1}, \tag{5}$$

$$\frac{d(\rho_{x_j} v_{x_j} A_{x_j})}{dt} l + \rho v^2 A|_{x=x_j+l/2} - \rho v^2 A|_{x=x_j-l/2} = A_{x_j}(p_j - p_{j-1}) -$$
$$- \frac{1}{2} \rho_{x_j} v_{x_j} |v_{x_j}| f_{x_j} S_{x_j} l - A_{x_j} \rho_{x_j} g \Delta z, \tag{6}$$

$$\frac{d(\bar{\rho}_j u_j A_j l)}{dt} - \dot{m}_{j+1} h_{x_j} - \dot{m}_j h_{x_{j-1}} = v_j A_j (p_{x_j} - p_{x_{j-1}}) + kA \left. \frac{\partial T}{\partial x} \right|_{x=x_j} - kA \left. \frac{\partial T}{\partial x} \right|_{x=x_{j-1}}. \tag{7}$$

Where, $l = L/n$, a certain λ_j value is the λ value in the jth control volume (V_j) and a certain λ_{x_r} value is the λ value for $x = x_r$.

These balance model is implemented in the pipe models of the ThermoFluid library in Modelica [Modelica Association (2007a)]. This paper presents a mean densities calculation method $\bar{\rho}_j$ based on [Casella (2006)], this mean density also affects the calculation of ρ_{x_j}.

5 Mean densities calculation

The Mean densities method is based on [Casella (2006)], but some changes are introduced due to a staggered grid has been considered in this work, instead of a collocated grid which was used in [Casella (2006)]. Mean densities allow to calculate thermodynamic properties for two-phase flow, especificaly density ρ and its partial derivatives, $\left.\frac{\partial\rho}{\partial h}\right|_p$ and $\left.\frac{\partial\rho}{\partial p}\right|_h$.

The mathematical model for the density thermodynamic properties [Casella (2006)] is based on the exact computation of the mean density in volumes where phase transitions occur, therefore avoiding non-physical artefacts due to the phase boundary crossing the discretization control volumes.

The calculation of the previously mentioned thermodynamic properties depends on different regions. These regions also depend on the flow state at the beginning (x_{j-1}) and at the end (x_j) of a control volume V_j (see Fig. 4), there are a total of 9 different regions shown in Tab. 1.

Table 1: Regions of mean densities

x_{j-1} \ x_j	Liquid	Two-phase	Steam
Liquid	1	3	6
Two-phase	8	2	4
Steam	9	7	5

The Mean densities method is intended to be used with energy-oriented applications, where thermo-hydraulic elements are involved, the pressure drop in components such as valves and turbines is much higher that in the evaporator itself, for that reason the pressure drop has been neglected in the evaporator, considering the pressure uniform in each control volume, $\tilde{p}$. It has been assumed, as a uniform pressure, the mean pressure between all the control volumes, Eq. 8.

$$\tilde{p} = \bar{p} = \frac{\sum_{j=1}^{n} p_j}{n}. \tag{8}$$

It is assumed that the variation of h is small enough that the specific enthalpy can be considered linearly distributed in the volume V. The uniform pressure is also needed to estimate specific enthalpy at the beginning and at the end of each control volume, h_{x_j} values in Fig. 5. Considering a collocated grid and a linearly distributed specific enthalpy, each h_{x_j} can be estimated using a linear interpolation between h_j

and h_{j+1}, Eq. 9. The particular cases, of the first and the last h values, h_{x_0} and h_{x_n}, can be estimated by using (h_1, h_2) values, Eq. 10, and (h_{n-1}, h_n) values, Eq. 11, in the linear interpolation respectively.

$$h_{x_j} = h_j + \frac{1}{2}(h_{j+1} - h_j), \quad j > 0 \wedge j < n, \tag{9}$$

$$h_{x_0} = h_1 - \frac{1}{2}(h_2 - h_1), \tag{10}$$

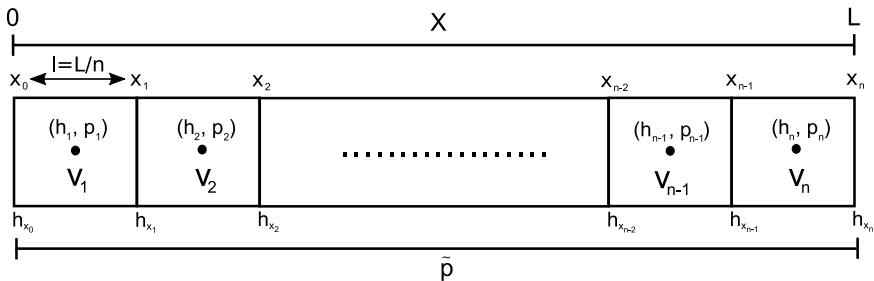$$h_{x_n} = h_n + \frac{3}{2}(h_n - h_{n-1}). \tag{11}$$

Figure 5: Finite volume method applied to volume V and calculation of $\tilde{p}$ and h_{x_j} values

Density in x_j can be calculated using IAPWS-IF97 standard, but being aware that the uniform pressure $\tilde{p}$ must be used, Eq. 12. The Modelica.Media library can be used for this purpose, in particular the Water.IF97_Utilities.rho_ph function from this library.

$$\rho_{x_j} = \rho(\tilde{p}, h_{x_j}). \tag{12}$$

5.1 Regions of Mean densities

Each region of mean densities in Tab. 1 is univocally defined by the state variables, pressure p and specific enthalpy h, due to the state variables define the flow state. In Tab. 2, Eq. 13 to Eq. 21 define the range of each region in the control volume V_j, using $\tilde{p}$, $h_{x_{j-1}}$ and h_{x_j}.

Where h_l and h_v are the specific enthalpy in the boiling and condensation curves respectively, using as pressure the uniform pressure $\tilde{p}$, Eq. 8.

Table 2: Range of the regions of mean densities

Region	Region range	
1	$h_{x_{j-1}} < h_l(\tilde{p}) \wedge h_{x_j} < h_l(\tilde{p})$	Eq. 13
2	$h_{x_{j-1}} \geq h_l(\tilde{p}) \wedge h_{x_{j-1}} \leq h_v(\tilde{p}) \wedge h_{x_j} \geq h_l(\tilde{p}) \wedge h_{x_j} \leq h_v(\tilde{p})$	Eq. 14
3	$h_{x_{j-1}} < h_l(\tilde{p}) \wedge h_{x_j} \geq h_l(\tilde{p}) \wedge h_{x_j} \leq h_v(\tilde{p})$	Eq. 15
4	$h_{x_{j-1}} \geq h_l(\tilde{p}) \wedge h_{x_{j-1}} \leq h_v(\tilde{p}) \wedge h_{x_j} > h_v(\tilde{p})$	Eq. 16
5	$h_{x_{j-1}} > h_v(\tilde{p}) \wedge h_{x_j} > h_v(\tilde{p})$	Eq. 17
6	$h_{x_{j-1}} < h_l(\tilde{p}) \wedge h_{x_j} > h_v(\tilde{p})$	Eq. 18
7	$h_{x_{j-1}} > h_v(\tilde{p}) \wedge h_{x_j} \geq h_l(\tilde{p}) \wedge h_{x_j} \leq h_v(\tilde{p})$	Eq. 19
8	$h_{x_{j-1}} \geq h_l(\tilde{p}) \wedge h_{x_{j-1}} \leq h_v(\tilde{p}) \wedge h_{x_j} < h_l(\tilde{p})$	Eq. 20
9	$h_{x_{j-1}} > h_v(\tilde{p}) \wedge h_{x_j} < h_l(\tilde{p})$	Eq. 21

5.2 Density calculation

Density calculation in mean densities is divided in regions 1-9 (Eq. 13-Eq. 21), where $\rho_{x_{j-1}}$ and ρ_{x_j} are calculated according to Eq. 12, h_l and h_v are calculated using as pressure the uniform pressure $\tilde{p}$, Eq. 8. The calculation procedure is analogous to the process described in [Casella (2006)].

Region 1 and 5: One-phase (Liquid/Liquid or Steam/Steam)

Considering a uniform pressure $\tilde{p}$, the density is then continuous and differentiable in these regions, hence for small variations of specific enthalpy h in V_j the density distribution can be assumed as a linear distribution, Eq. 22.

$$\bar{\rho}_j = \frac{1}{l} \int\limits_{(j-1)l}^{jl} \rho \, dx = \frac{\rho_{x_{j-1}} + \rho_{x_j}}{2}. \tag{22}$$

Region 2: Two-phase / Two-phase

Density is also continuous and differentiable in this region, but it can double its value across a small distance if the pressure is low and if the specific enthalpy is just over the h_l curve. Consider the mass fraction x_v (Eq. 23) of the steam in the two-phase flow and v the specific volume (Eq. 24), being v_l the specfic enthalpy at h_l and v_v the specific enthalpy at h_v.

$$x_v = \frac{h_{x_j} - h_l}{h_v - h_l}, \tag{23}$$

$$v = x_v v_v + (1 - x_v)v_l = \frac{1}{h_v - h_l}[h_{x_j}(v_v - v_l) + h_v v_l + h_l v_v]. \tag{24}$$

Replacing Eq. 24 in Eq. 23, Eq. 25 is obtained.

$$v = x_v v_v + (1 - x_v)v_l = \frac{1}{h_v - h_l}[h_{x_j}(v_v - v_l) + h_v v_l + h_l v_v]. \tag{25}$$

Isolating h, Eq. 26 is obtained.

$$h = \frac{v(h_v - h_l) - h_v v_l - h_l v_v}{v_v - v_l}. \tag{26}$$

Calculating $h_{x_j} - h_{x_{j-1}}$ from Eq. 26, Eq. 27 is obtained.

$$h_{x_j} - h_{x_{j-1}} = \frac{h_v - h_l}{v_v - v_l}(v_{x_j} - v_{x_{j-1}}). \tag{27}$$

Assuming a linear specific enthalpy distribution, due to h is linear with respect to x and v es linear with respect to h, the mean density in this region is represented by Eq. 28.

$$
\begin{aligned}
\bar{\rho}_j &= \frac{1}{l}\int_{(j-1)l}^{jl} \rho \, dx = \frac{1}{h_{x_j} - h_{x_{j-1}}}\int_{h_{x_{j-1}}}^{h_{x_j}} \rho \, dh = \frac{1}{h_{x_j} - h_{x_{j-1}}}\frac{h_v - h_l}{v_v - v_l}\int_{v_{x_{j-1}}}^{v_{x_j}} \frac{1}{v} \, dv = \\
&= \frac{1}{h_{x_j} - h_{x_{j-1}}}\frac{h_v - h_l}{v_v - v_l}\left(\ln\left(v_{x_j}\right) - \ln(v_{x_{j-1}})\right) = \\
&= \frac{1}{h_{x_j} - h_{x_{j-1}}}\frac{h_v - h_l}{v_v - v_l}\ln\left(\frac{\rho_{x_{j-1}}}{\rho_{x_j}}\right).
\end{aligned}
\tag{28}
$$

Note that Eq. 28 becomes singular when $h_{x_{j-1}} = h_{x_j}$, hence it is necessary to check if the difference between both terms in the previous equation is smaller that a certain threshold ε, Eq. 29.

$$
\begin{aligned}
\bar{\rho}_j &= \frac{1}{h_{x_j} - h_{x_{j-1}}}\frac{h_v - h_l}{v_v - v_l}\ln\left(\frac{\rho_{x_{j-1}}}{\rho_{x_j}}\right), \quad |h_{j+1} - h_j| \geq \varepsilon, \\
\bar{\rho}_j &= \rho_{x_{j-1}}, \quad |h_{x_j} - h_{x_{j-1}}| < \varepsilon.
\end{aligned}
\tag{29}
$$

Region 3: Liquid / Two-phase

In this region, the density has a discontinuous derivative due to the phase change in the boiling curve h_l, the mean density can be calculated splitting the integral in two parts, liquid - two-phase, using Eq. 22 and Eq. 29, obtaining therefore Eq. 30.

$$
\begin{aligned}
\bar{\rho}_j &= \frac{1}{l} \int_{(j-1)l}^{jl} \rho \, dx = \frac{1}{h_{x_j} - h_{x_{j-1}}} \int_{h_{x_{j-1}}}^{h_{x_j}} \rho \, dh = \\
&= \frac{1}{h_{x_j} - h_{x_{j-1}}} \left[\int_{h_{x_{j-1}}}^{h_l} \rho \, dh + \int_{h_l}^{h_{x_j}} \rho \, dh \right] = \\
&= \frac{1}{h_{x_j} - h_{x_{j-1}}} \left[\frac{\rho_{x_{j-1}} - \rho_l}{2} (h_l - h_{x_{j-1}}) + \frac{h_v - h_l}{v_v - v_l} \ln\left(\frac{\rho_l}{\rho_{x_j}} \right) \right].
\end{aligned}
\tag{30}
$$

The $h_{x_j} = h_{x_{j-1}}$ case is not possible due to Eq. 15.

Region 4: Two-phase / Steam

Splitting the integral in two parts, two-phase - steam, using Eq. 29 and Eq. 22, Eq. 31 is obtained.

$$
\begin{aligned}
\bar{\rho}_j &= \frac{1}{h_{x_j} - h_{x_{j-1}}} \left[\int_{h_{x_{j-1}}}^{h_v} \rho \, dh + \int_{h_v}^{h_{x_j}} \rho \, dh \right] = \\
&= \frac{1}{h_{x_j} - h_{x_{j-1}}} \left[\frac{h_v - h_l}{v_v - v_l} \ln\left(\frac{\rho_{x_{j-1}}}{\rho_v} \right) + \frac{\rho_v + \rho_{x_j}}{2} (h_{x_j} - h_v) \right].
\end{aligned}
\tag{31}
$$

The $h_{x_j} = h_{x_{j-1}}$ case is not possible due to Eq. 16.

Region 6: Liquid / Steam

Splitting the integral in three parts, liquid - two-phase - steam, using Eq. 22, Eq. 29 and Eq. 22 again, Eq. 32 is obtained.

$$
\bar{\rho}_j = \frac{1}{h_{x_j} - h_{x_{j-1}}} \left[\int_{h_{x_{j-1}}}^{h_l} \rho \, dh + \int_{h_l}^{h_v} \rho \, dh + \int_{h_v}^{h_{x_j}} \rho \, dh \right] = \frac{1}{h_{x_j} - h_{x_{j-1}}} \cdot
$$
$$
\cdot \left[\frac{\rho_{x_{j-1}} + \rho_l}{2} (h_l - h_{x_{j-1}}) + \frac{h_v - h_l}{v_v - v_l} \ln \left(\frac{\rho_l}{\rho_v} \right) + \frac{\rho_v + \rho_{x_j}}{2} (h_{x_j} - h_v) \right].
$$
(32)

The $h_{x_j} = h_{x_{j-1}}$ case is not possible due to Eq. 18.

Region 7: Steam / Two-phase

Splitting the integral in two parts, steam - two-phase, using Eq. 22 and Eq. 29, Eq. 33 is obtained.

$$
\bar{\rho}_j = \frac{1}{h_{x_j} - h_{x_{j-1}}} \left[\int_{h_{x_{j-1}}}^{h_v} \rho \, dh + \int_{h_v}^{h_{x_j}} \rho \, dh \right] =
$$
$$
= \frac{1}{h_{x_j} - h_{x_{j-1}}} \left[\frac{\rho_{x_{j-1}} + \rho_v}{2} (h_v - h_{x_{j-1}}) + \frac{h_v - h_l}{v_v - v_l} \ln \left(\frac{\rho_v}{\rho_{x_j}} \right) \right].
$$
(33)

The $h_{x_j} = h_{x_{j-1}}$ case is not possible due to Eq. 19.

Region 8: Two-phase / Liquid

Splitting the integral in two parts, two-phase - liquid, using Eq. 29 and Eq. 22, Eq. 34 is obtained.

$$
\bar{\rho}_j = \frac{1}{h_{x_j} - h_{x_{j-1}}} \left[\int_{h_{x_{j-1}}}^{h_l} \rho \, dh + \int_{h_l}^{h_{x_j}} \rho \, dh \right] =
$$
$$
= \frac{1}{h_{x_j} - h_{x_{j-1}}} \left[\frac{h_v - h_l}{v_v - v_l} \ln \left(\frac{\rho_{x_{j-1}}}{\rho_l} \right) + \frac{\rho_l + \rho_{x_j}}{2} (h_{x_j} - h_l) \right].
$$
(34)

The $h_{x_j} = h_{x_{j-1}}$ case is not possible due to Eq. 20.

Region 9: Steam / Liquid

Splitting the integral in three parts, steam - two-phase - liquid, using Eq. 22, Eq. 29 and Eq. 22 again, Eq. 35 is obtained.

$$\bar{\rho}_j = \frac{1}{h_{x_j} - h_{x_{j-1}}} \left[\int_{h_{x_{j-1}}}^{h_v} \rho \, dh + \int_{h_v}^{h_l} \rho \, dh + \int_{h_l}^{h_{x_j}} \rho \, dh \right] = \frac{1}{h_{x_j} - h_{x_{j-1}}} \cdot$$

$$\cdot \left[\frac{\rho_{x_{j-1}} + \rho_v}{2} (h_v - h_{x_{j-1}}) + \frac{h_v - h_l}{v_v - v_l} \ln \left(\frac{\rho_v}{\rho_l} \right) + \frac{\rho_l + \rho_{x_j}}{2} (h_{x_j} - h_l) \right]. \tag{35}$$

The $h_{x_j} = h_{x_{j-1}}$ case is not possible due to Eq. 21.

5.3 $\left. \frac{\partial \rho}{\partial h} \right|_p$ *calculation*

This partial derivative can be calculated independently of the mean densities region, as it is shown in Eq. 36 [Casella (2006)].

$$\left. \frac{\partial \bar{\rho}_j}{\partial h} \right|_p = \frac{\partial}{\partial h} \left(\frac{1}{l} \int_{(j-1)l}^{jl} \rho(p, h(x)) \, dx \right) = \frac{1}{l} \int_{(j-1)l}^{jl} \frac{\partial}{\partial h} \rho(p, h(x)) \, dx =$$

$$= \frac{1}{l} \int_{(j-1)l}^{jl} \frac{\partial}{\partial x} \frac{dx}{dh} \rho(p, h(x)) \, dx = \frac{1}{l} \frac{l}{h_{x_j} - h_{x_{j-1}}} \int_{(j-1)l}^{jl} \frac{\partial \rho}{\partial x} \, dx = \tag{36}$$

$$= \frac{\rho_{x_j} - \rho_{x_{j-1}}}{h_{x_j} - h_{x_{j-1}}}.$$

Note that Eq. 36 becomes sigular when $h_{x_{j-1}} = h_{x_j}$, hence it is necessary to check if the difference between both terms is smaller that a certain threshold ε, Eq. 37.

$$\left. \frac{\partial \bar{\rho}_j}{\partial h} \right|_p = \frac{\rho_{x_j} - \rho_{x_{j-1}}}{h_{x_j} - h_{x_{j-1}}}, \quad |h_{x_j} - h_{x_{j-1}}| \geq \varepsilon,$$

$$\left. \frac{\partial \bar{\rho}_j}{\partial h} \right|_p = \left. \frac{\partial \bar{\rho}_{x_{j-1}}}{\partial h} \right|_p, \quad |h_{x_j} - h_{x_{j-1}}| < \varepsilon. \tag{37}$$

5.4 $\left. \frac{\partial \rho}{\partial p} \right|_h$ *calculation*

This partial derivate can be calculated directly from the equations defined in section 5.2, the next subsections show the partial derivative for each mean densities region. The calculation of this partial derivate involves calculating some thermodynamic

properties in x_{j-1} and x_j, these thermodynamic properties can be calculated using a suitable fluid library, in Modelica language the Modelica.Media library can be used for that purpose, always being aware that when a pressure value is needed for the calculation, the uniform pressure $\tilde{p}$ must be used.

Region 1 and 5: One-phase (Liquid/Liquid or Steam/Steam)

The partial derivative of Eq. 22 with respect to pressure keeping specific enthalpy constant is Eq. 38.

$$\left.\frac{\partial \bar{\rho}_j}{\partial p}\right|_h = \frac{1}{2}\left(\left.\frac{\partial \rho_{x_{j-1}}}{\partial p}\right|_h + \left.\frac{\partial \rho_{x_j}}{\partial p}\right|_h\right). \tag{38}$$

Region 2: Two-phase / Two-phase

The partial derivative of Eq. 23 with respect to pressure keeping specific enthalpy constant is Eq. 39.

$$\begin{aligned}
\left.\frac{\partial \bar{\rho}_j}{\partial p}\right|_h &= \frac{1}{(h_{x_j} - h_{x_{j-1}})(v_l - v_v)^2}\left(\ln\left(\frac{\rho_{x_{j-1}}}{\rho_{x_j}}\right)(v_v - v_l)\left(\frac{\partial h_v}{\partial p} - \frac{\partial h_l}{\partial p}\right)\right. \\
&\quad + \frac{(h_l - h_v)(\rho_l - \rho_v)\left(-\rho_{x_j}\left.\frac{\partial \rho_{x_{j-1}}}{\partial p}\right|_h + \rho_{x_j}\left.\frac{\partial \rho_{x_j}}{\partial p}\right|_h\right)}{\rho_{x_{j-1}}\rho_{x_j}\rho_l\rho_v} \\
&\quad \left. - \ln\left(\frac{\rho_{x_{j-1}}}{\rho_{x_j}}\right)(h_v - h_l)\left(\frac{\frac{\partial \rho_l}{\partial p}}{\rho_l^2} - \frac{\frac{\partial \rho_v}{\partial p}}{\rho_v^2}\right)\right).
\end{aligned} \tag{39}$$

Region 3: Liquid / Two-phase

The partial derivative of Eq. 24 with respect to pressure keeping specific enthalpy constant is Eq. 40.

$$
\begin{aligned}
\left.\frac{\partial \bar{\rho}_j}{\partial p}\right|_h = \frac{1}{h_{x_j} - h_{x_{j-1}}} & \left(\frac{1}{2}(\rho_{x_{j-1}} + \rho_l)\frac{\partial h_l}{\partial p} + \frac{\ln\left(\frac{\rho_l}{\rho_{x_{j-1}}}\right)\left(-\frac{\partial h_l}{\partial p} + \frac{\partial h_v}{\partial p}\right)}{v_v - v_l} \right. \\
& + \frac{1}{2}(h_l - h_{x_{j-1}})\left(\left.\frac{\partial \rho_{x_{j-1}}}{\partial p}\right|_h + \frac{\partial \rho_l}{\partial p}\right) + \frac{(h_l - h_v)\rho_v\left(\rho_l \left.\frac{\partial \rho_{x_j}}{\partial p}\right|_h - \rho_{x_j}\frac{\partial \rho_l}{\partial p}\right)}{\rho_{x_j}(\rho_l - \rho_v)} \\
& \left. + \frac{\ln\left(\frac{\rho_l}{\rho_{x_j}}\right)(h_l - h_v)\left(\rho_v^2 \frac{\partial \rho_l}{\partial p} - \rho_l^2 \frac{\partial \rho_v}{\partial p}\right)}{(\rho_l - \rho_v)^2} \right).
\end{aligned}
\tag{40}
$$

Region 4: Two-phase / Steam

The partial derivative of Eq. 25 with respect to pressure keeping specific enthalpy constant is Eq. 41.

$$
\begin{aligned}
\left.\frac{\partial \bar{\rho}_j}{\partial p}\right|_h = \frac{1}{h_{x_j} - h_{x_{j-1}}} & \left(-\frac{1}{2}(\rho_{x_j} + \rho_v)\frac{\partial h_v}{\partial p} + \frac{\ln\left(\frac{\rho_{x_{j-1}}}{\rho_v}\right)\left(\frac{\partial h_v}{\partial p} - \frac{\partial h_l}{\partial p}\right)}{v_v - v_l} \right. \\
& + \frac{(h_{x_j} - h_v)\left(\left.\frac{\partial \rho_{x_j}}{\partial p}\right|_h + \frac{\partial \rho_v}{\partial p}\right)}{2} + \frac{(h_l - h_v)\rho_l\left(\rho_{x_{j-1}}\frac{\partial \rho_v}{\partial p} - \rho_v \left.\frac{\partial \rho_{x_{j-1}}}{\partial p}\right|_h\right)}{\rho_{x_{j-1}}(\rho_l - \rho_v)} \\
& \left. + \frac{\ln\left(\frac{\rho_{x_{j-1}}}{\rho_v}\right)(h_l - h_v)\left(\rho_v^2 \frac{\partial \rho_l}{\partial p} - \rho_l^2 \frac{\partial \rho_v}{\partial p}\right)}{(\rho_l - \rho_v)^2} \right).
\end{aligned}
\tag{41}
$$

Region 6: Liquid / Steam

The partial derivative of Eq. 26 with respect to pressure keeping specific enthalpy constant is Eq. 42.

$$
\begin{aligned}
\left.\frac{\partial \bar{\rho}_j}{\partial p}\right|_h &= \frac{1}{2(h_{x_j} - h_{x_{j-1}})} \left((\rho_{x_{j-1}} + \rho_l)\frac{\partial h_l}{\partial p} - (\rho_{x_j} + \rho_v)\frac{\partial h_v}{\partial p} \right. \\
&+ \frac{2\ln\left(\frac{\rho_l}{\rho_v}\right)\left(\frac{\partial h_l}{\partial p} + \frac{\partial h_v}{\partial p}\right)}{v_v - v_l} + (h_l - h_{x_{j-1}})\left(\left.\frac{\partial \rho_{x_{j-1}}}{\partial p}\right|_h + \frac{\partial \rho_l}{\partial p}\right) \\
&+ (h_{x_j} - h_v)\left(\left.\frac{\partial \rho_{x_j}}{\partial p}\right|_h + \frac{\partial \rho_v}{\partial p}\right) + \frac{2(h_l - h_v)\left(\rho_l \frac{\partial \rho_v}{\partial p} - \rho_v \frac{\partial \rho_l}{\partial p}\right)}{\rho_l - \rho_v} \\
&+ \left. \frac{2\ln\left(\frac{\rho_l}{\rho_v}\right)(h_l - h_v)\left(\rho_v^2 \frac{\partial \rho_l}{\partial p} - \rho_l^2 \frac{\partial \rho_v}{\partial p}\right)}{(\rho_l - \rho_v)^2} \right).
\end{aligned}
\tag{42}
$$

Region 7: Steam / Two-phase

The partial derivative of Eq. 27 with respect to pressure keeping specific enthalpy constant is Eq. 43.

$$
\begin{aligned}
\left.\frac{\partial \bar{\rho}_j}{\partial p}\right|_h &= \frac{1}{h_{x_j} - h_{x_{j-1}}} \left(\frac{1}{2}(\rho_{x_{j-1}} + \rho_v)\frac{\partial h_v}{\partial p} + \frac{\ln\left(\frac{\rho_v}{\rho_{x_j}}\right)\left(\frac{\partial h_v}{\partial p} - \frac{\partial h_l}{\partial p}\right)}{v_v - v_l} \right. \\
&+ \frac{(h_v - h_{x_{j-1}})\left(\left.\frac{\partial \rho_{x_{j-1}}}{\partial p}\right|_h + \frac{\partial \rho_v}{\partial p}\right)}{2} + \frac{(h_l - h_v)\rho_l\left(\rho_v \left.\frac{\partial \rho_{x_j}}{\partial p}\right|_h - \rho_{x_j}\frac{\partial \rho_v}{\partial p}\right)}{\rho_{x_j}(\rho_l - \rho_v)} \\
&+ \left. \frac{\ln\left(\frac{\rho_v}{\rho_{x_j}}\right)(h_l - h_v)\left(\rho_v^2 \frac{\partial \rho_l}{\partial p} - \rho_l^2 \frac{\partial \rho_v}{\partial p}\right)}{(\rho_l - \rho_v)^2} \right).
\end{aligned}
\tag{43}
$$

Region 8: Two-phase / Liquid

The partial derivative of Eq. 28 with respect to pressure keeping specific enthalpy constant is Eq. 44.

$$\left.\frac{\partial \bar{\rho}_j}{\partial p}\right|_h = \frac{1}{h_{x_j} - h_{x_{j-1}}} \left(-\frac{1}{2}(\rho_{x_j} + \rho_l)\frac{\partial h_l}{\partial p} + \frac{\ln\left(\frac{\rho_{x_{j-1}}}{\rho_l}\right)\left(\frac{\partial h_v}{\partial p} - \frac{\partial h_l}{\partial p}\right)}{v_v - v_l} \right.$$

$$+ \frac{1}{2}(h_{x_j} - h_l)\left(\left.\frac{\partial \rho_{x_j}}{\partial p}\right|_h + \frac{\partial \rho_l}{\partial p}\right) + \frac{(h_l - h_v)\rho_v\left(\rho_{x_{j-1}}\frac{\partial \rho_l}{\partial p} - \rho_l \left.\frac{\partial \rho_{x_{j-1}}}{\partial p}\right|_h\right)}{\rho_{x_{j-1}}(\rho_l - \rho_v)}$$

$$\left. + \frac{\ln\left(\frac{\rho_{x_{j-1}}}{\rho_l}\right)(h_l - h_v)\left(\rho_v^2 \frac{\partial \rho_l}{\partial p} - \rho_l^2 \frac{\partial \rho_v}{\partial p}\right)}{(\rho_l - \rho_v)^2} \right).$$

$$(44)$$

Region 9: Steam / Liquid

The partial derivative of Eq. 29 with respect to pressure keeping specific enthalpy constant is Eq. 45.

$$\left.\frac{\partial \bar{\rho}_j}{\partial p}\right|_h = \frac{1}{2(h_{x_j} - h_{x_{j-1}})} \left((\rho_{x_{j-1}} + \rho_v)\frac{\partial h_v}{\partial p} - (\rho_{x_j} + \rho_l)\frac{\partial h_l}{\partial p} \right.$$

$$+ \frac{2\ln\left(\frac{\rho_v}{\rho_l}\right)\left(\frac{\partial h_v}{\partial p} - \frac{\partial h_l}{\partial p}\right)}{v_v - v_l} + (h_{x_{j-1}} - h_l)\left(\left.\frac{\partial \rho_{x_j}}{\partial p}\right|_h + \frac{\partial \rho_l}{\partial p}\right)$$

$$+ (h_v - h_{x_{j-1}})\left(\left.\frac{\partial \rho_{x_{j-1}}}{\partial p}\right|_h + \frac{\partial \rho_v}{\partial p}\right) + \frac{2(h_l - h_v)\left(\rho_v \frac{\partial \rho_l}{\partial p} - \rho_l \frac{\partial \rho_v}{\partial p}\right)}{\rho_l - \rho_v}$$

$$\left. + \frac{2\ln\left(\frac{\rho_v}{\rho_l}\right)(h_l - h_v)\left(\rho_v^2 \frac{\partial \rho_l}{\partial p} - \rho_l^2 \frac{\partial \rho_v}{\partial p}\right)}{(\rho_l - \rho_v)^2} \right).$$

$$(45)$$

6 Modelica implementation

The mean densities mathematical model has been implemented using Modelica, for that purpose a library, called CIEMAT_Water_MeanDensities, has been developed. This library includes all the functions, classes and models required. The central element of this library is the pipe model, PipeDD_MeanDensities which requires a medium model, MeanDensities_WaterSteamMedium_ph and also a thermodynamic properties computation function called Ciemat_MeanDensities_ph. These three main elements of the library are detailed below.

- **Thermodynamic properties computation function.** This function calculates the thermodynamic properties values as a function of the state variables (p,h). ρ, $\left.\frac{\partial \rho}{\partial h}\right|_p$ and $\left.\frac{\partial \rho}{\partial p}\right|_h$ are calculated using the mean densities mathematical model, the rest of the thermodynamic properties involved in the model are calculated using functions from the Modelica.Media library.

- **Medium model.** The medium model uses the previously mentioned function for the calculation of the thermodynamic properties in each control volume of the pipe. This medium model and the abovementioned function refers to a steam-water two-phase flow. It is based on ThermalModel_ph.Medium from the ThermoFluid library.

- **Pipe model.**   The rigid pipe volume is discretized in control volumes using the finite volume method (FVM) and the staggered grid method, using a medium model which calculates the thermodynamic properties for each control volume. This model is based on PipeDD model from the ThermoFluid library.

Fig. 6 and 7 show the developed Modelica library which implements the mean densities model. Serveral example models have been implemented for testing the library and also for comparison and validation against the ThermoFluid and Modelica.Media models.
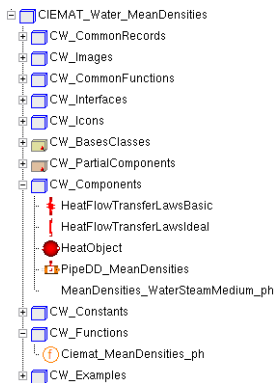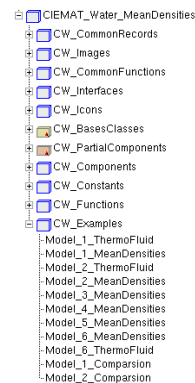

Figure 6: Library components   Figure 7: Library examples

7   Simulation

A simple boiler pipe Modelica model is presented in this section as an example to focus attention on the chattering problem. The Modelica component diagram is

shown in Fig. 8. It has a sinusoidal heat source equally distributed through a pipe discretized into 10 control volumes. Fig. 9 shows the heat source in a 1000-second simulation. The input water flow is constant (0.36 l/s) and it is pumped through the heated pipe. As the heat increases, the boiling barrier moves from the end of the pipe toward the beginning and viceversa.
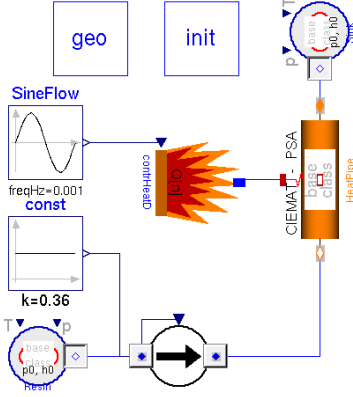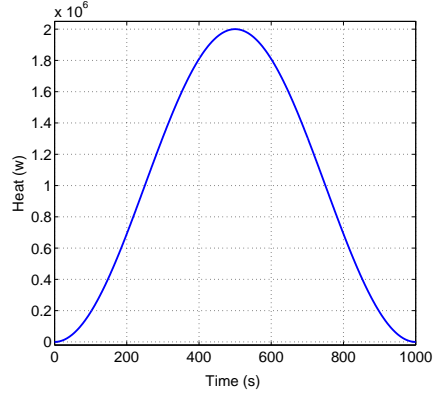

Figure 8: Boiler pipe model

Figure 9: Sinusoidal heat source

Analysing the simulation results, the time instants which trigger the events can be identified, moreover other information can be obtained as it is shown in Tab. 3. Each of these time instants, where a large amount of events are triggered, are the time instants where chattering problems appear in simulation. It can be seen in Tab. 3 that chattering problems appear in phase transtions that correspond to the boiling and condensation curves.

Table 3: Chattering time instants in simulation

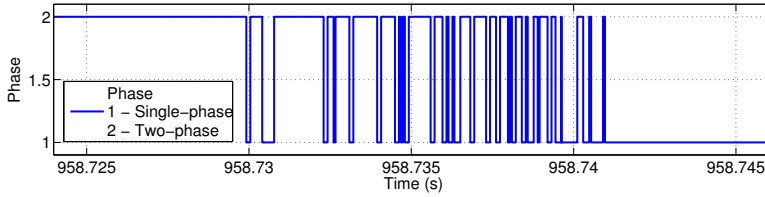| Simulation Time	Control Volume	Phase Transition
632.96	CV 5	Two-phase flow→Superheated steam
833.08	CV 4	Two-phase flow→Subcooled liquid
865.58	CV 5	Two-phase flow→Subcooled liquid
890.12	CV 6	Two-phase flow→Subcooled liquid
910.97	CV 7	Two-phase flow→Subcooled liquid
932.07	CV 8	Two-phase flow→Subcooled liquid
958.73	CV 9	Two-phase flow→Subcooled liquid

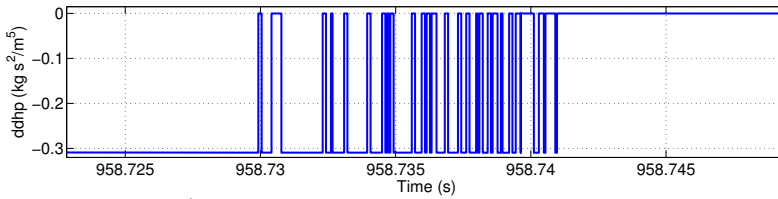Figure 10: Phase changes, 9th control volume, boiling curve, chattering time

Figure 11: $\left.\dfrac{\partial \rho}{\partial h}\right|_{p}$, 9th control volume, boiling curve, chattering time

The chattering effects can be clearly seen in simulation. For instance, focusing in the 9th control volume, Fig. 10 shows the transitions between the single and two-phase regions (1 for single and 2 for two-phase region), also all the thermodynamic properties have high frequency oscillations due to the repeated phase changes when the chattering problem appears in simulation, for instance Fig. 11 shows $\left.\dfrac{\partial \rho}{\partial h}\right|_{p}$ in the 9th control volume when the chattering problem appears.

7.1 Simulation results

DASSL [Petzold (1986)] has been the solver used in the dynamic simulation, the absolute and relative tolerances are both 10^{-4} and the sampling time was set to 1 second, obtaining equidistant output data for each simulated second, the number of output intervals is therefore 1000. It can be seen the large amount of state events which increases the simulation time considerably because each event restarts the integration process. Tab. 4 summarizes the simulation results, the original model uses the ThermoFluid library whereas the other model uses the Mean densities library. It can be seen how the state events have been completely wiped out, from 9147 to 0 in the mean densities model, and this happens because the thermodynamic properties models are continuous and differentiable in the mean densities approach, for that reason a crossed function at phase changes is not required. As a result of these smooth models, the simulation time has been reduced considerably

from 36.5 to 2.3 seconds, this is a reduction of 93.7% in the simulation time.

Table 4: Simulation results

Parameter	Original Model	Mean densities
Simulated time (s)	1,000	1,000
CPU integration time (s)	36.5	2.3
State events	9,147	0
Min. integration stepsize	$5.18 \cdot 10^{-7}$	$1.31 \cdot 10^{-5}$
Max. integration stepsize	23.2	26.9
Max. integration order	5	4
Chattering	Yes	No

It can be clearly seen in Fig. 13 that there is no chattering in the mean densities approach. Both Fig. 12 and 13 show the velocity state vector fields ($v(h, p)$) in the 9th control volume when the chattering problem appears in simulation (in the boiling curve h') for the original model and mean densities model respectively. Fig. 12 shows repeated phase changes which are the cause of the reduction in the simulator performance increasing the simulation time, because each phase change is managed by a crossed function which stops and resumes the simulation process. On the contrary Fig. 13 shows that there is no confrotation between velocity state vectors, due to the thermodynamic properties are smooth, the transition between phases just happens, there is no need of a crossed function and therefore this approach reduces the simulation time needed.
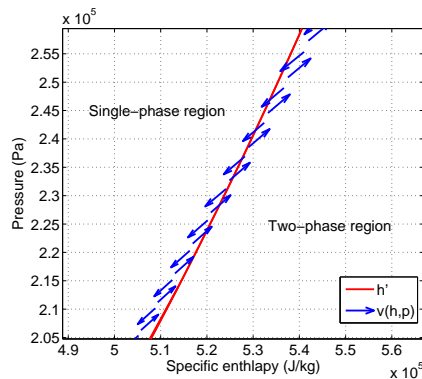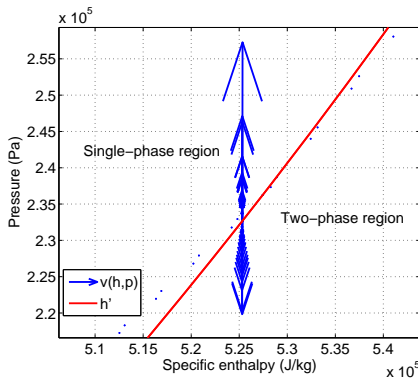

Figure 12: Velocity state vector field, original model, 9th CV

Figure 13: Velocity state vector field, mean densities model, 9th CV

Fig. 14 shows a comparison between density values in the 9th control volume obtained from the original model and the mean densities model. It can be seen how the mean densities model follows correctly the original model dynamic. Fig. 15 shows the different mean densities regions used during simulation in the 9th control volume.

Eq. 46 defines the percentual relative error, where V_o is a variable in the original model and V_{md} is the same variable in the mean densities approach. The maximum percentual relative error committed by the mean densities approach in the output specific enthlapy of the pipe is only 0.33%, meanwhile the maximum percentual relative error committed in density in steady state is higher due to the use of a uniform pressure and the linear interpolation among specific enthalphy values, the maximum error is up to 17%, at phase changes the error commited is slightly higher, this is understable due to the mean densities approach defines smooth models for the thermodynamic properties.

$$\varepsilon_r(V_{md}) = 100 \cdot \frac{|V_{md} - V_o|}{V_o} \tag{46}$$

Quantifying the gain in speed and the error in general are difficult tasks:

1. The ODE system is still a nonlinear system after applying the Mean density method. However, the ODE coefficients are smoother, this causes that the coefficient gradients are lower in amplitude. Due to the fact that the numerical integrators are complex, the evaluation of the simulation computational load can only be done comparing the simulation time for both simulations, using and not using the Mean density approach.

2. The Mean densities approach uses a mean pressure along the volume, the only practical way of knowing the maximum error committed is to perform two simulations, setting as the pressure: the input and the output pressure. That give us an error band, so all the thermodynamic properties (i.e. density, specific enthalpy) can be subtracted (from both simulation) and that is the maximum error committed by the Mean density simulation in that thermodynamic property.

8   Conclusions and future work

The mean densities method applied to a steam-water two-phase flow mathematical model which uses a finite volume method and a staggered grid has been presented in
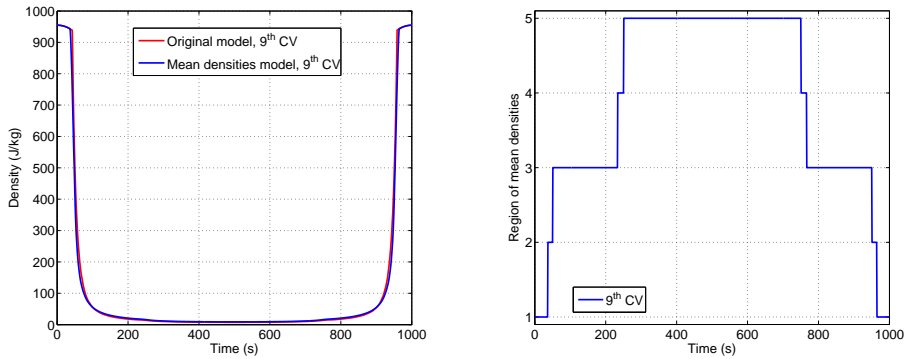
Figure 14: Density comparison in the 9th CV

Figure 15: Different regions of mean densities used in the 9th CV

this paper. The mean densities method is based on a uniform pressure, in this case a mean pressure, and on a mean density value in each control volume. The pressure drop in the evaporator has been neglected due to the Mean densities approach is intended to be used for energy-oriented applications involving thermo-hydraulic components, and in that case the pressure drop in other elements such as valves and turbines in much higher than in the evaporator itself. This method has been applied to a staggered grid using a linear interpolation between specific enthalpy in nearby control volumes to obtain specific enthalpy values at control volume boundaries, which allows the calculation of a mean density value in each control volume. Also the density partial derivatives with respect to the state variables, specific enthalpy and pressure, have been obtained.

The main advantage of this method is that it wipes out the chattering problem, due to the continuous and differentiable modelling of density and its partial derivatives, which leads to faster simulations and increases the simulation performance. The error committed is low in terms of the output variable of a volume, such as the specific enthalpy, although the error committed in density is higher due to use a uniform pressure, a linear interpolation for the specific enthalpy and the mean density concept, however the method is worthy and this error can be assumed. The principal future goal is to model complex real systems using this new library, such as to develop a new DISS test facility Modelica model which will take advantage of the new free of chattering developed library.

References

Anderson, J. (1995): *Computational Fluid Dynamics*. McGraw-Hill Science / Engineering / Math.

Casella, F. (2006): Object-oriented modelling of two-phase fluid flows by the finite volume method. In *5th Mathmod Vienna*.

Eborn, J. (2001): *On Model Libraries for Thermohydraulic Applications*. PhD thesis, Department of Automatic Control, Lund Institute of Technology, Lund, Sweden, 2001.

Elmqvist, H.; Tummescheit, H.; Otter, M. (2003): Object-oriented modeling of thermo-fluid systems. In *Proceedings of the Third International Modelica Conference*, pp. 269–286, Linköping, Sweden. Modelica Association and Linköping University, Sweden.

Harlow, F. H.; Welch, E. J. (1965): Numerical calculation of time-dependent viscous incompressible flow of fluid with free surface. *Physics of Fluids*, vol. 8, no. 12, pp. 2182–2189.

Heusser, P. A. (1996): *Modelling and Simulation of Boiling Channels with a General Front Tracking Approach*. PhD thesis, Diss. Techn. Wiss. ETH Zürich, 1996.

IAPWS (1997): Release on the IAPWS Industrial Formulation 1997 for the Termodynamic Properties of Water and Steam. Technical report, The International Association for the Properties of Water and Steam, Erlangen, Germany, 1997.

Kutshcer, C.; Davenport, R.; Dougherty, D.; Gee, R.; Masterson, P.; Kenneth, E. (1982): Design approaches for solar industrial process-heat system. Tech. rep. seri/tr-253-1356, Solar Energy Research Institute, Golden (Colorado), USA, 1982.

Modelica Association (2007): Modelica Language Specification 2.2.1, 2007a.

Modelica Association (2007): Modelica Media Library 2.2.1, 2007b.

Patankar, S. V. (1980): *Numerical Heat Transfer and Fluid Flow*. Hemisphere, Washington,D.C.

Petzold, L. R. (1986): A description of DASSL: a differential/algebraic system solver. Technical report, Sandia Labs, Livermore, CA, 1986.

Rhie, C. M.; Chow, W. L. (1983): Numerical study of the turbulent flow past an airfoil with trailing edge separation. *AIAA Journal*, vol. 21, pp. 1525–1532.

Roberts, P. (2000): Simulation of industrial processes for control engineers [book reviews]. *Computing & Control Engineering Journal*, vol. 11, no. 2, pp. 52–52.

The American Society of Mechanical Engineers (1999): Rebuilding steam tables. *Mechanical Engineering*, vol. 121, no. 3, pp. 78–111.

Tummescheit, H. (2002): *Design and Implementation of Object-Oriented Model Libraries using Modelica.* PhD thesis, Department of Automatic control, Lund Institute of Technology, Lund, Sweden, 2002.

Tummescheit, H.; Eborn, J.; Wagner, F. (2000): Development of a modelica base library for modeling of thermo-hydraulic systems.. In Association, M.(Ed): *Modelica 2000 Workshop Proceedings*, Lund.

Yebra, L. (2006): *Object-Oriented Modelling of Parabolic-Trough Collectors with Modelica (in Spanish).* PhD thesis, Universidad Nacional de Educación a Distancia (UNED), Madrid, Spain, 2006.

Zarza, E. (2000): *The Direct Steam Generation with Parabolic Collectors. The DISS project (in Spanish).* PhD thesis, Escuela Superior de Ingenieros Industriales de Sevilla, Seville, Spain, 2000.